Published in final edited form as:
Curr Mol Med. 2013 December ; 13(10): 1538–1548.

Multimodality Imaging of CXCR4 in Cancer: Current Status towards Clinical Translation

Tapas R. Nayak[1], **Hao Hong**[1], **Yin Zhang**[2], and **Weibo Cai**[1,2,3]

[1]Department of Radiology, University of Wisconsin - Madison, WI, USA

[2]Department of Medical Physics, University of Wisconsin - Madison, WI, USA

[3]University of Wisconsin Carbone Cancer Centre, Madison, WI, USA

Abstract

CXCR4 has gained tremendous attention over the last decade, since it was found to be up-regulated in a wide variety of cancer types, in addition to its role in human immunodeficiency virus infection. Molecular imaging of CXCR4 with small molecules, peptides, and antibodies has been a vibrant research area over the last several years. In this review article, we will summarize the current status of imaging CXCR4 with fluorescence, bioluminescence, positron emission tomography, and single-photon emission computed tomography techniques. Since each molecular imaging modality has its own strengths and weaknesses, dual-modality probes that can be detected by more than one imaging techniques have also been investigated. Non-invasive visualization of CXCR4 expression has potential clinical applications in multiple facets of patient management. While big strides have been made over the last several years in the development of CXCR4-targeted imaging probes, clinical translation and investigation of these agents in cancer patients are eagerly awaited. Since CXCR4 is also involved in many other diseases beyond cancer, these clinically translatable probes can also play multiple roles in other pathological disorders such as myocardial infarction and several immunodeficiency disorders.

Keywords

CXCR4; molecular imaging; positron emission tomography (PET); metastasis; chemokine receptor; chemokine; cancer

INTRODUCTION

Chemokine receptors, which interact with specific types of cytokines known as chemokines, play diverse roles in cytoskeletal rearrangement, cell adhesion, and directional migration [1, 2]. To date, approximately 50 chemokines and 20 chemokine receptors have been identified [3]. Both the chemokines and chemokine receptors have been classified into four distinct groups (CXC, CX3C, CC, and C), based on the amino acid sequence around the first two cysteine residues within the chemokine, which typically contains four invariant cysteine residues [4]. Generally, the names of chemokines contain “L” and an identifying number (e.g. CCL1 belongs to the chemokine subfamily “CC” with number “1”), whereas the names of chemokine receptors contain “R” and an identifying number (e.g. CCR1 belongs to the chemokine receptor subfamily “CC” with number “1”) [5].

Requests for reprints: Weibo Cai, PhD, Departments of Radiology and Medical Physics, University of Wisconsin - Madison, Room 7137, 1111 Highland Avenue, Madison, WI 53705-2275, USA, wcai@uwhealth.org; Phone: 608-262-1749; Fax: 608-265-0614.

Chemokines and their interaction with specific chemokine receptors are involved in tumor development/metastasis [6], as well as many other diseases such as atherosclerosis [7], autoimmune disorders [8], neurodegenerative processes [9], and human immunodeficiency virus (HIV) infection [10, 11]. In particular, CXCR4 and its only endogenous ligand known as the stromal derived factor 1 (SDF-1, also called CXCL12) have gained tremendous attention over the last decade, since CXCR4 was found to be up-regulated in a wide variety of cancer types including breast, prostate, lung, bladder, ovarian, renal, oesophageal, colorectal, and pancreatic cancer, lymphoma, melanoma, osteosarcoma, neuroblastoma, etc. [1, 12–14]. In the following text of this review, the terms SDF-1 and CXCL12 will be used interchangeably. Furthermore, high level of CXCR4 expression correlated with tumor progression/metastasis [15, 16], as well as poor prognosis and resistance to chemotherapy [17, 18]. Because of its prominent role in cancer biology, CXCR4 is an attractive target for not only therapeutic but also molecular imaging applications, which can potentially be used to predict tumor behaviour and evaluate the therapeutic responses to standard chemotherapy and novel molecularly targeted therapies.

MOLECULAR IMAGING OF CXCR4

The interdisciplinary field of molecular imaging has witnessed tremendous advances over the last decade, not only in clinical/preclinical oncology [19–25] but also in many other disciplines such as regenerative medicine [26, 27]. Molecular imaging of CXCR4 with small molecules, peptides, and antibodies has been a vibrant research area over the last several years, which can enable non-invasive detection of CXCR4 expression during tumor development/metastasis, as well as potentially many other scenarios such as stem cell mobilization and anti-HIV activity. A brief summary of these studies is shown in Table 1, which includes fluorescence, bioluminescence, positron emission tomography (PET), and single-photon emission computed tomography (SPECT). The CXCR4 antagonists/agonists that have been explored can be divided into four major categories: peptidic CXCR4 antagonists, non-peptidic CXCR4 antagonists, anti-CXCR4 antibodies, and recombinant SDF-1/CXCL12 [28]. Several excellent review articles are available in the literature regarding CXCR4 and its antagonists [28–31]. Herein we will only briefly describe the use of these four classes of agents for imaging purposes.

In several early studies, a small group of peptide-based CXCR4 antagonists (e.g. T22, T134, and T140) were identified and synthesized for their anti-HIV activities [32–34]. Among these peptides, T140 (i.e. Arg^{1}-Arg^{2}-Nal^{3}-*cyclo*(Cys^{4}-Tyr^{5}-Arg^{6}-Lys^{7}-D-Lys8-Pro9-Tyr10-Arg^{11}-Cit^{12}-Cys^{13})-Arg^{14}) was considered to be the most active CXCR4 antagonist, which can inhibit the binding of an anti-CXCR4 monoclonal antibody (mAb) to CXCR4 [33]. However, T140 exhibited poor metabolic stability due to the cleavage of the C-terminal Arg residue. Subsequently, several derivatives of T140 (e.g. 4-F-benzoyl-TN14003, Ac-TZ14011, and TY14003) were constructed which are currently under investigation. In addition, certain metabolically stable cyclic pentapeptides (e.g. FC131 and CPCR4-2) that were based on T140 are also being investigated for imaging applications [35].

A series of bicyclams synthesized in the early 1990s were found to be potent and selective inhibitors of CXCR4 [36, 37]. In this class of CXCR4 inhibitors, AMD3100 and AMD3465 have been investigated as imaging probes [38, 39]. Several other cyclam derivatives with CXCR4 antagonistic activity (e.g. AMD070 and KRH-1636) are primarily being investigated for their anti-HIV activities and will not be discussed in this review.

Antibodies that bind to human CXCR4 or SDF-1 have been reported to inhibit metastases and progression of several cancer types in preclinical models [40–43]. However, few anti-CXCR4 antibodies have been explored for molecular imaging and/or immunotherapy of

cancer, which may be partly attributed to the conformational heterogeneity exhibited by CXCR4 [29].

SDF-1 exists in alpha and beta forms due to alternative splicing of the same gene [44]. In many studies, SDF-1 is used in competition experiments to confirm the binding affinity/specificity of the antagonists. In some cases, SDF-1 was also conjugated to certain image tag and investigated as molecular imaging probes. In addition, peptidic analogs of SDF-1 (e.g. CTCE-9908 and CTCE-0214 which exhibit inhibitory and agonist activity of CXCR4, respectively) are also being utilized for cancer therapy [28].

Since each molecular imaging modality has its own strengths and weaknesses, dual-modality probes that can be detected by more than one imaging techniques have also been investigated. The mounting preclinical data, withstanding further research pertaining to novel agents for non-invasive imaging of CXCR4, may allow for real-time and quantitative evaluation of CXCR4 expression in both primary tumors and metastatic nodules, which can be used to effectively guide interventions tailored to individual patients for personalized treatment of cancer. In the remaining sections of this review article, we will summarize the current status of imaging CXCR4 expression using different techniques.

FLUORESCENCE IMAGING OF CXCR4

Fluorescence imaging techniques have been widely used in biomedical research. The three most commonly used classes of fluorophores are fluorescent proteins, organic dyes, and quantum dots. Because of the relatively low cost, fluorescence imaging of various cancer markers have been intensively studied in cell culture and small animal models. In clinical settings, fluorescence imaging can be used for detecting lesions close to the skin surface (e.g. breast cancer imaging) and/or tissues accessible by endoscopy (such as malignant lesions in the esophagus and colon), as well as for intra-operative visualization (i.e. image-guided surgery). A number of reports exist in the literature on fluorescence imaging of CXCR4.

In an early study, SDF-1 was labelled with fluorescein for the detection of CXCR4-dependent internalization of SDF-1 by stromal bone marrow cells [45], which significantly facilitated the evaluation of CXCR4 activation. In another report, Ac-TZ14011 was labelled with fluorescein or AlexaFluor 488, at the D-Lys^{8} ε-amino group of the peptide [46]. The resulting probes displayed specificity and high affinity for CXCR4 *in vitro* (Fig. (1A)). TAMRA- or fluorescein-labelled Ac-TZ14011 have also been analyzed for their CXCR4 binding activity *in vitro* [47]. It was concluded that such fluorescence-based ligand binding assays could be useful in identification and investigation of novel pharmacophores for CXCR4 binding.

Recently, fluorescein-labelled Ac-TZ14011 was demonstrated to be capable of differentiating tumor cells with high (e.g. MDA-MB-231^{CXCR4+}) and low (e.g. wild-type MDA-MB-231) CXCR4 expression [48], which may be useful to determine differential CXCR4 expression levels in various tissues and the tumor with immunohistochemistry. In another report by the same group, Ac-TZ14011 was conjugated to a luminescent iridium dye for visualizing CXCR4 expression in tumor cells [49]. TY14003 (i.e. Ac-Arg-Arg-Nal-Cys-Tyr-Cit-Arg-D-Lys-Pro-Tyr-Arg-Cit-Cys-Arg-NH_2), another derivative of the T140 peptide, has been labelled with carboxyfluorescein at the D-Lys residue for detection of CXCR4 expression in a N-butyl-N-(4-hydroxybutyl)nitrosamine-induced bladder cancer model [50], which demonstrated its potential as a diagnostic tool to visualize small or flat high-grade superficial bladder cancer.

In one report, metal nanoshells have been covalently labelled with anti-CXCR4 mAbs for targeting CXCR4 on the cell surface [51]. The fluorescence signal observed by time resolved confocal microscopy not only displayed strong emission intensity and distinct lifetime, which could be readily separated from cellular autofluorescence, but also allowed for quantitation of CXCR4 level on the cell surface.

Most of the abovementioned studies were carried out in cell culture, where the fluorophore used emit in the visible range. For *in vivo* applications, imaging in the near-infrared (NIR, 700–900 nm) window is desirable since both tissue absorption and autofluorescence are very low within this range [52, 53]. In a recent report, CXCL12 was conjugated with an NIR dye (IRDye 800CW) and evaluated for CXCR4-targeted cancer detection with fluorescence imaging [54]. After investigating the selectivity, sensitivity, and biological activity of the conjugates *in vitro*, where fluorescence signal of the conjugates was detectable in both the A764 human glioma cells and MCF7 human breast cancer cells that express CXCR4, *in vivo* studies revealed that subcutaneous MCF7 and A764 tumors in immunodeficient mice could also be detected with high sensitivity (Fig. (1B)). On the other hand, control conjugates such as fluorescently labelled bovine serum albumin or lactalbumin were not able to detect the tumors, which suggested CXCR4 specificity of the fluorescently labelled CXCL12 *in vivo*.

Guiding surgery with molecularly targeted fluorescent agents has attracted enormous interests over the last decade. Recently, a proof-of-principle study investigating the potential benefit of intra-operative tumor-specific fluorescence imaging in staging and debulking surgery for ovarian cancer was reported, using a systemically administered targeted fluorescent agent (folate-FITC which binds to the folate receptor, overexpressed on most ovarian cancer cells) [55]. Because of the pivotal role of CXCL12/CXCR4 signaling in tumor metastasis [56, 57], intra-operative imaging of CXCR4 may be very useful in guiding tumor resection, especially in the metastatic setting where imaging of CXCR4 may be able to identify small metastatic tumor nodules during surgery to improve the clinical outcome. The use of an NIR dye, which has much better signal penetration in an imaging window with significantly less autofluorescence than a dye that emits in the visible range, is more desirable for surgical guidance with the development of suitable intra-operative imaging systems.

BIOLUMINESCENCE IMAGING OF CXCR4

Because of very low background signal and high sensitivity, bioluminescence imaging (BLI) has been widely used in preclinical research. The fact that no additional excitation light will be needed in BLI is highly advantageous for reducing the background signal. To date, only a few examples of imaging CXCR4 with BLI have been reported. Different from the other imaging techniques that have been investigated for CXCR4, BLI typically detects the interaction between CXCR4 and other proteins/peptides rather than the expression of CXCR4 itself.

By detecting the interaction between CXCR4 and β-arrestin through a firefly luciferase (FLuc)-based complementation assay, CXCR4 signalling was visualized and quantified in intact cells and living mice [58]. In the presence of CXCL12, dose-dependent increase in BLI signal was observed using this reporter system. In addition, the BLI signal could be effectively blocked by specific inhibitors of CXCR4 signalling, which suggested its suitability for *in vivo* imaging of CXCR4 activation. In a follow-up study, this reporter system was also used to detect and quantify the conformational changes in receptor complexes in an orthotopic xenograft model of breast cancer [59]. The BLI signal was found to be specific for homodimeric conformation of CXCR4 but not its heterodimer form with CXCR7, another chemokine receptor that is also involved in tumor growth and metastasis.

Meanwhile, another reporter system based on a fusion protein that consists of CXCL12 and Gaussia luciferase (GLuc) was developed for cellular studies of CXCR4 and CXCR7 [60]. Fusion to CXCL12 did not alter the bioluminescence spectrum of GLuc, which also exhibited minimal effect on its function under varying conditions of pH, temperature, and NaCl concentration.

Recently, a GLuc fragment complementation strategy was developed to quantify the binding of CXCL12 to CXCR4 and CXCR7 [61]. Similar to other enzyme complementation assays where the enzyme was split into the N-terminal half and the C-terminal half, binding of CXCL12-CGLuc to NGLuc-CXCR4 or NGLuc-CXCR7 (where CGLuc and NGLuc denote the two parts of the GLuc enzyme) reconstitutes GLuc and produces light as a quantitative measure of the ligand-receptor binding (Fig. (2)). BLI revealed CXCL12-CXCR7 binding in primary and metastatic tumors in a mouse model of breast cancer. Furthermore, this technique was also employed to quantify drug-mediated inhibition of CXCL12-CXCR4 binding in living mice.

In another study, this split reporter system was used to investigate CXCL12-CXCR4 signalling in ovarian cancer and to interrogate the effects of inhibiting this pathway on tumor progression and survival [62]. After demonstrating that the split reporter system could detect the binding of CXCL12 to CXCR4 and quantify specific inhibition of such interaction *in vitro*, CXCL12-CXCR4 binding and inhibition was monitored in a xenograft model of metastatic human ovarian cancer by imaging GLuc complementation and, in the meantime, assessing tumor progression with FLuc. Loss of GLuc signal was observed after inhibition of CXCL12-CXCR4 binding by AMD3100, which also had modest improvement on the survival rate in mice with metastatic ovarian cancer.

In a subsequent report, a similar dual-luciferase system involving both GLuc and FLuc was used to investigate CXCR7-dependent scavenging of CXCL12 in breast tumors *in vivo* [63], which provided useful insight on how this can affect tumor growth and metastasis of a separate co-implanted population of $CXCR4^+$ breast cancer cells. These abovementioned reports on BLI imaging of CXCR4 with various strategies/luciferases demonstrated that imaging of CXCR4 interaction with other proteins/ligands (e.g. CXCL12) can not only shed light on intercellular signalling during tumor development and metastasis, but also help the development of novel therapeutic agents that target these interactions.

PET IMAGING OF CXCR4

PET is a non-invasive nuclear medicine imaging technique which utilizes positron-emitting tracers to obtain a three dimensional image [64]. Currently, ^{18}F-FDG is widely used in clinical oncology [65, 66], while many other PET tracers are under preclinical/clinical investigation [19, 67–69]. Some of the commonly used PET isotopes include ^{11}C ($t_{1/2}$: 20 min), ^{18}F ($t_{1/2}$: 110 min), 64Cu ($t_{1/2}$: 12.8 h), 68Ga ($t_{1/2}$: 68 min), 13N ($t_{1/2}$: 10 min), 15O ($t_{1/2}$: 2 min), ^{86}Y ($t_{1/2}$: 14.7 h), 89Zr ($t_{1/2}$: 3.3 d), and 124I ($t_{1/2}$: 4.2 d).

Since AMD3100 is a potent inhibitor of CXCR4 [37, 70, 71], it has been labelled with ^{64}Cu and evaluated for PET imaging of CXCR4 *in vivo* [38]. The binding affinity to CXCR4 was determined to be in the micromolar range, which was not affected by incorporation of Cu^{2+}. Biodistribution studies in normal mice showed specific accumulation of ^{64}Cu-AMD3100 in organs and tissues that express CXCR4. Subsequently, ^{64}Cu-AMD3100 was evaluated in tumor models, where the retention and uptake of the tracer in subcutaneous tumors derived from U87 glioblastoma cell lines with high or low CXCR4 expression was compared [39]. A six-fold increase in tracer uptake was observed in tumors derived from U87 cells that were stably transfected with CXCR4 (i.e. U87-stb-CXCR4) than the wild-type U87 tumors. In addition, similar findings were also observed in several other tumor models, such as

orthotopic breast tumor xenografts and breast cancer lung metastasis models, thereby demonstrating the broad potential applications for PET imaging of CXCR4 in cancer. In a recent report, ^{64}Cu-AMD3100 was also investigated for PET imaging of CXCR4 in various mouse tumor models [72].

Similar to the abovementioned studies on AMD3100, another high affinity CXCR4 antagonist called AMD3465 has also been labelled with ^{64}Cu and evaluated as a PET tracer in subcutaneous U87, U87-stb-CXCR4, and colon HT-29 tumors (Fig. (3)) [73]. *In vivo* PET imaging and *ex vivo* biodistribution studies suggested better specificity, target selectivity, and tumor-to-muscle ratio for ^{64}Cu-AMD3465 than that of ^{64}Cu-AMD3100. Although these studies suggested potential clinical applications of both ^{64}Cu-AMD3100 and ^{64}Cu-AMD3465 in visualizing CXCR4 expressing tumors, there are many concerns for this class of PET tracers that need to be addressed in future studies: prominent tracer uptake and accumulation in the liver and certain other tissues (which is likely due to CXCR4-independent factors such as plasma protein binding of AMD3100 and AMD 3465), instability of ^{64}Cu that was bound to the ligand, metabolism of the tracers, among others.

In addition to these small molecule CXCR4 antagonists, highly selective peptidic antagonists of CXCR4 such as 4-F-benzoyl-TN14003 (4-F-T140) have also been labelled with ^{18}F and evaluated *in vivo* for their potential in imaging CXCR4 expression with PET [74]. It was found that 4-^{18}F-T140 bound specifically to red blood cells both *in vitro* and *in vivo*, which could be blocked by a small amount of “cold” 4-F-T140 to give higher tracer uptake in CXCR4 expressing tumors. PET studies demonstrated clear visualization of CXCR4 positive but not CXCR4 negative tumors.

Another T140-based PET tracer was developed, by ^{64}Cu-labelling through the chelator DOTA (1,4,7,10-tetraazacyclododecane-1,4,7,10-tetraacetic acid), which enabled imaging of CXCR4 expressing tumors [75]. However, this tracer also exhibited high accumulation in the metabolic organs such as liver and kidneys. In a later study, DOTA-T140 was labelled with ^{68}Ga and investigated in cell-based studies [76]. To eliminate binding and accumulation at undesired sites, two other T140-based tracers called NOTA-NFB and DOTA-NFB were developed, which were demonstrated to specifically accumulate in CXCR4 positive tumor xenografts and allow for clear visualization of CXCR4 expression by PET [77].

Recently, a pentapeptide called CPCR4-2 that binds to CXCR4 was conjugated to DOTA and labelled with ^{68}Ga [35]. ^{68}Ga-CPCR4-2 exhibited high CXCR4 binding affinity with persistent tumor uptake, which resulted in PET imaging of CXCR4 expressing tumors and metastases with good contrast, even for those in the hepatic and abdominal region [78]. Interestingly, very low accumulation and retention of the tracer was observed in the kidneys. Subsequently, a library of analogs of these cyclic pentapeptide have been synthesized as potential imaging agent [79]. However, *in vivo* data has not been reported yet.

SPECT IMAGING OF CXCR4

SPECT is another widely used nuclear medicine imaging technique in the clinic [80, 81]. However, the sensitivity of SPECT is at least an order of magnitude lower than PET. In addition, although the special resolution for small animal SPECT is higher than PET, the resolution of clinical SPECT is significant lower than clinical PET. Because of the wide availability of SPECT isotopes such as ^{99m}Tc ($t_{1/2}$: 6.0 h), 111In ($t_{1/2}$: 2.8 d), and radioiodine, SPECT imaging in cancer has been intensively studied since it does not require heavy infrastructure such as a cyclotron.

DTPA (i.e. diethylene triamine pentaacetic acid) conjugated Ac-TZ14011 was synthesized and labelled with ^{111}In for SPECT imaging in anima tumor models, which showed high accumulation in CXCR4 expressing tumors with relatively low blood radioactivity level and background signal in normal tissues such as the muscle [82]. In a follow-up study, this tracer was used to visualize CXCR4 expression in a mammary intraepithelial neoplastic outgrowth (MIN-O) mouse tumor model, which resembles human ductal carcinoma *in situ* (DCIS) [83]. Tracer uptake in early MIN-O lesions was found to be significantly lower than in larger and late stage lesions, which was corroborated by the degree of membranous CXCR4 staining as evidenced by histology.

An anti-human CXCR4 mAb called 12G5 was labelled with ^{125}I for SPECT/CT imaging of CXCR4 expression in an experimental U87 brain tumor model [84]. Clear and specific accumulation of radioactivity in the tumor was observed within 24 hours post-injection, which was gradually cleared by 72 hours post-injection (Fig. (4)). The maximum tumor-to-non-tumor contrast was achieved at 48 hours post-injection. Since radioiodine can freely diffuse across the cellular membrane after the mAb is internalized upon CXCR4 binding and subsequently degraded, future use of a residualizing radiometal as the image label is expected to increase the tumor uptake and retention of radioactivity.

In an interesting report, SDF-1α was labelled with ^{99m}Tc and investigated for imaging and quantification of CXCR4 expression levels in myocardial infarction [85]. It was found that the tracer displayed high affinity and specificity for endogenous CXCR4. Since the key characteristics of molecular imaging is that it is molecular specific instead of disease specific, the same imaging agent may play important roles in multiple diseases where CXCR4 expression is up-regulated. Much future effort should be directed towards imaging CXCR4 expression beyond cancer.

DUAL-MODALITY IMAGING OF CXCR4

Among the abovementioned techniques for imaging of CXCR4 which include fluorescence, bioluminescence, PET, and SPECT, each modality has its limitations. Therefore, a combination of multiple modalities may be needed to gather more information and to facilitate future clinical translation. For example, PET/SPECT imaging can be used for non-invasive whole-body imaging, while fluorescence imaging can be used to guide surgical procedures for tumor removal. Recently, a dual-modality imaging agent was synthesized by conjugating Ac-TZ14011 with both DTPA (for ^{111}In labelling) and a CyAL-5.5 dye [86]. Flow cytometry and confocal microscopy studies showed that the dual-labelled peptide exhibited specific CXCR4 binding, comparable to that of the mono-functionalized peptide derivatives. *In vivo* SPECT/CT and fluorescence studies showed good tumor uptake of the tracer. Furthermore, potential use of this dual-labelled agent for image-guided surgery was also demonstrated in mouse models.

In a follow-up study, dendrimers containing monomeric, dimeric, and tetrameric Ac-TZ14011 were labelled using the same strategy and compared *in vivo*, where the dimer and tetramer had considerably higher tumor uptake than the monomer [87]. In addition, biodistribution studies revealed that the additional peptides in the dimer and tetramer also reduced non-specific muscle uptake. Since SPECT has much lower sensitivity than PET, future development of a dual-modality PET/fluorescence agent for the imaging of CXCR4 expression should be investigated.

CONCLUSION AND FUTURE PERSPECTIVES

CXCR4 and its crucial roles in tumor development and metastasis have been confirmed by a large number of literature reports and mounting preclinical/clinical evidence. To date, an

array of targeting ligands have been investigated for imaging of CXCR4 expression in cancer, ranging from small molecule and peptide-based agents (~1 kDa) to full-size antibodies (~150 kDa). The imaging modalities used includes both radionuclide-based (i.e. SPECT and PET) and optical (both fluorescence and bioluminescence) techniques. In a few reports, combination of two imaging modalities has also been demonstrated [86, 87], which deserves more research effort in the near future.

Visualization of CXCR4 expression has potential clinical applications in many aspects: cancer diagnosis where lesions/metastases with high CXCR4 expression can be detected; patient stratification where patients with high CXCR4 expression can be selected for CXCR4-targeted therapies/clinical trials; treatment monitoring where non-invasive imaging of CXCR4 expression can indicate the therapeutic response; facilitating new anti-cancer drug development through monitoring the therapeutic efficacy of various drugs that target the CXCR4 signaling pathway; guiding surgical removal of primary/metastatic lesions with fluorescently labeled agents that bind specifically to CXCR4 *in vivo*, among others. Quantitative correlation of CXCR4 expression level with PET/SPECT tracer uptake is highly desirable for future treatment monitoring applications, where the biological changes during therapeutic intervention can be non-invasively and quantitatively assessed in each individual patient.

Much future effort should be directed towards the development of clinically translatable CXCR4-targeted imaging agents. Although a wide variety of imaging probes for CXCR4 have been synthesized and investigated over the last several years, an ideal agent with minimal synthetic procedure and optimal selectivity/specificity for CXCR4 *in vivo* (both primary tumors and metastatic lesions) has not been developed yet. For example, peptidic antagonists of CXCR4 typically exhibit poor metabolic stability and may be difficult to synthesize at low cost. Bicyclams can be readily synthesized but their prominent uptake in the liver and normal tissues is a major concern. The use of peptoids, which are composed of N-substituted glycines, may be more advantageous for non-invasive imaging applications [88]. Antibodies are typically very specific for their antigens, however the longer circulation half-lives limit the tumor-to-non-tumor contrast for imaging applications. Development of antibody fragments which retain the antigen-binding affinity/specificity with much faster blood clearance may be more suitable for imaging applications than radiolabeled intact antibodies [89].

Because of their excellent sensitivity and tissue penetration, radionuclide-based imaging techniques possess much higher clinical potential than non-radionuclide-based techniques. Many challenges need to be addressed in preclinical and clinical models before clinical translation of CXCR4-targeted imaging probes enter clinical investigation. Big strides have been made over the last several years towards molecular imaging of CXCR4, clinical translation and investigation of optimal CXCR4-targeted imaging probes in cancer patients are eagerly awaited. Since CXCR4 is involved in many other diseases beyond cancer, these probes may also play multiple roles in other diseases such as myocardial infarction and several immunodeficiency disorders.

Acknowledgments

This work is supported, in part, by the University of Wisconsin - Madison, the National Institutes of Health (NIBIB/NCI 1R01CA169365), the Department of Defense (W81XWH-11-1-0644), and the American Cancer Society (RSG-13-099-01-CCE).

References

1. Muller A, Homey B, Soto H, et al. Involvement of chemokine receptors in breast cancer metastasis. Nature. 2001; 410:50–6. [PubMed: 11242036]
2. Murphy PM. International Union of Pharmacology. XXX. Update on chemokine receptor nomenclature. Pharmacol Rev. 2002; 54:227–9. [PubMed: 12037138]
3. Allen SJ, Crown SE, Handel TM. Chemokine: receptor structure, interactions, and antagonism. Annu Rev Immunol. 2007; 25:787–820. [PubMed: 17291188]
4. Fernandez EJ, Lolis E. Structure, function, and inhibition of chemokines. Annu Rev Pharmacol Toxicol. 2002; 42:469–99. [PubMed: 11807180]
5. Bacon K, Baggiolini M, Broxmeyer H, et al. Chemokine/chemokine receptor nomenclature. J Interferon Cytokine Res. 2002; 22:1067–8. [PubMed: 12433287]
6. Vandercappellen J, Van Damme J, Struyf S. The role of CXC chemokines and their receptors in cancer. Cancer Lett. 2008; 267:226–44. [PubMed: 18579287]
7. Braunersreuther V, Mach F, Steffens S. The specific role of chemokines in atherosclerosis. Thromb Haemost. 2007; 97:714–21. [PubMed: 17479181]
8. Iwamoto T, Okamoto H, Toyama Y, Momohara S. Molecular aspects of rheumatoid arthritis: chemokines in the joints of patients. FEBS J. 2008; 275:4448–55. [PubMed: 18662305]
9. Mines M, Ding Y, Fan GH. The many roles of chemokine receptors in neurodegenerative disorders: emerging new therapeutical strategies. Curr Med Chem. 2007; 14:2456–70. [PubMed: 17979699]
10. De Clercq E. Inhibition of HIV infection by bicyclams, highly potent and specific CXCR4 antagonists. Mol Pharmacol. 2000; 57:833–9. [PubMed: 10779364]
11. Fujii N, Nakashima H, Tamamura H. The therapeutic potential of CXCR4 antagonists in the treatment of HIV. Expert Opin Investig Drugs. 2003; 12:185–95.
12. Kang H, Watkins G, Douglas-Jones A, Mansel RE, Jiang WG. The elevated level of CXCR4 is correlated with nodal metastasis of human breast cancer. Breast. 2005; 14:360–7. [PubMed: 16216737]
13. Balkwill F. The significance of cancer cell expression of the chemokine receptor CXCR4. Semin Cancer Biol. 2004; 14:171–9. [PubMed: 15246052]
14. Kulbe H, Levinson NR, Balkwill F, Wilson JL. The chemokine network in cancer--much more than directing cell movement. Int J Dev Biol. 2004; 48:489–96. [PubMed: 15349823]
15. Yoon Y, Liang Z, Zhang X, et al. CXC chemokine receptor-4 antagonist blocks both growth of primary tumor and metastasis of head and neck cancer in xenograft mouse models. Cancer Res. 2007; 67:7518–24. [PubMed: 17671223]
16. Li JK, Yu L, Shen Y, et al. Inhibition of CXCR4 activity with AMD3100 decreases invasion of human colorectal cancer cells in vitro. World J Gastroenterol. 2008; 14:2308–13. [PubMed: 18416455]
17. Zeng Z, Samudio IJ, Munsell M, et al. Inhibition of CXCR4 with the novel RCP168 peptide overcomes stroma-mediated chemoresistance in chronic and acute leukemias. Mol Cancer Ther. 2006; 5:3113–21. [PubMed: 17172414]
18. Oda Y, Tateishi N, Matono H, et al. Chemokine receptor CXCR4 expression is correlated with VEGF expression and poor survival in soft-tissue sarcoma. Int J Cancer. 2009; 124:1852–9. [PubMed: 19107931]
19. Alauddin MM. Positron emission tomography (PET) imaging with ^{18}F-based radiotracers. Am J Nucl Med Mol Imaging. 2012; 2:55–76. [PubMed: 23133802]
20. Eary JF, Hawkins DS, Rodler ET, Conrad EUI. ^{18}F-FDG PET in sarcoma treatment response imaging. Am J Nucl Med Mol Imaging. 2011; 1:47–53. [PubMed: 23133794]
21. Hong H, Zhang Y, Sun J, Cai W. Positron emission tomography imaging of prostate cancer. Amino Acids. 2009; 39:11–27. [PubMed: 19946787]
22. Hong H, Zhang Y, Sun J, Cai W. Molecular imaging and therapy of cancer with radiolabeled nanoparticles. Nano Today. 2009; 4:399–413. [PubMed: 20161038]
23. Grassi I, Nanni C, Allegri V, et al. The clinical use of PET with ^{11}C-acetate. Am J Nucl Med Mol Imaging. 2012; 2:33–47. [PubMed: 23133801]

24. Vach W, Høilund-Carlsen PF, Fischer BM, Gerke O, Weber W. How to study optimal timing of PET/CT for monitoring of cancer treatment. Am J Nucl Med Mol Imaging. 2011; 1:54–62. [PubMed: 23133795]
25. Wang RE, Niu Y, Wu H, Amin MN, Cai J. Development of NGR peptide-based agents for tumor imaging. Am J Nucl Med Mol Imaging. 2011; 1:36–46. [PubMed: 23133793]
26. Hong H, Yang Y, Zhang Y, Cai W. Non-invasive imaging of human embryonic stem cells. Curr Pharm Biotechnol. 2010; 11:685–92. [PubMed: 20497109]
27. Cai W, Zhang Y, Kamp TJ. Imaging of induced pluripotent stem cells: from cellular reprogramming to transplantation. Am J Nucl Med Mol Imaging. 2011; 1:18–28. [PubMed: 21841970]
28. Burger JA, Peled A. CXCR4 antagonists: targeting the microenvironment in leukemia and other cancers. Leukemia. 2009; 23:43–52. [PubMed: 18987663]
29. Baribaud F, Edwards TG, Sharron M, et al. Antigenically distinct conformations of CXCR4. J Virol. 2001; 75:8957–67. [PubMed: 11533159]
30. Wong D, Korz W. Translating an antagonist of chemokine receptor CXCR4: from bench to bedside. Clin Cancer Res. 2008; 14:7975–80. [PubMed: 19088012]
31. Teicher BA, Fricker SP. CXCL12 (SDF-1)/CXCR4 pathway in cancer. Clin Cancer Res. 2010; 16:2927–31. [PubMed: 20484021]
32. Masuda M, Nakashima H, Ueda T, et al. A novel anti-HIV synthetic peptide, T-22 ([Tyr5,12,Lys7]-polyphemusin II). Biochem Biophys Res Commun. 1992; 189:845–50. [PubMed: 1472056]
33. Tamamura H, Xu Y, Hattori T, et al. A low-molecular-weight inhibitor against the chemokine receptor CXCR4: a strong anti-HIV peptide T140. Biochem Biophys Res Commun. 1998; 253:877–82. [PubMed: 9918823]
34. Tchou I, Misery L, Sabido O, et al. Functional HIV CXCR4 coreceptor on human epithelial Langerhans cells and infection by HIV strain X4. J Leukoc Biol. 2001; 70:313–21. [PubMed: 11493625]
35. Demmer O, Gourni E, Schumacher U, Kessler H, Wester HJ. PET imaging of CXCR4 receptors in cancer by a new optimized ligand. ChemMedChem. 2011; 6:1789–91. [PubMed: 21780290]
36. De Clercq E, Yamamoto N, Pauwels R, et al. Potent and selective inhibition of human immunodeficiency virus (HIV)-1 and HIV-2 replication by a class of bicyclams interacting with a viral uncoating event. Proc Natl Acad Sci USA. 1992; 89:5286–90. [PubMed: 1608936]
37. De Clercq E. The bicyclam AMD3100 story. Nat Rev Drug Discov. 2003; 2:581–7. [PubMed: 12815382]
38. Jacobson O, Weiss ID, Szajek L, Farber JM, Kiesewetter DO. ^{64}Cu-AMD3100--a novel imaging agent for targeting chemokine receptor CXCR4. Bioorg Med Chem. 2009; 17:1486–93. [PubMed: 19188071]
39. Nimmagadda S, Pullambhatla M, Stone K, et al. Molecular imaging of CXCR4 receptor expression in human cancer xenografts with [^{64}Cu]AMD3100 positron emission tomography. Cancer Res. 2010; 70:3935–44. [PubMed: 20460522]
40. Phillips RJ, Burdick MD, Lutz M, et al. The stromal derived factor-1/CXCL12-CXC chemokine receptor 4 biological axis in non-small cell lung cancer metastases. Am J Respir Crit Care Med. 2003; 167:1676–86. [PubMed: 12626353]
41. Chen GS, Yu HS, Lan CC, et al. CXC chemokine receptor CXCR4 expression enhances tumorigenesis and angiogenesis of basal cell carcinoma. Br J Dermatol. 2006; 154:910–8. [PubMed: 16634895]
42. Engl T, Relja B, Marian D, et al. CXCR4 chemokine receptor mediates prostate tumor cell adhesion through alpha5 and beta3 integrins. Neoplasia. 2006; 8:290–301. [PubMed: 16756721]
43. Bertolini F, Dell'Agnola C, Mancuso P, et al. CXCR4 neutralization, a novel therapeutic approach for non-Hodgkin's lymphoma. Cancer Res. 2002; 62:3106–12. [PubMed: 12036921]
44. De La Luz Sierra M, Yang F, Narazaki M, et al. Differential processing of stromal-derived factor-1alpha and stromal-derived factor-1beta explains functional diversity. Blood. 2004; 103:2452–9. [PubMed: 14525775]

45. Dar A, Goichberg P, Shinder V, et al. Chemokine receptor CXCR4-dependent internalization and resecretion of functional chemokine SDF-1 by bone marrow endothelial and stromal cells. Nat Immunol. 2005; 6:1038–46. [PubMed: 16170318]
46. Oishi S, Masuda R, Evans B, et al. Synthesis and application of fluorescein- and biotin-labeled molecular probes for the chemokine receptor CXCR4. Chembiochem. 2008; 9:1154–8. [PubMed: 18412193]
47. Nomura W, Tanabe Y, Tsutsumi H, et al. Fluorophore labeling enables imaging and evaluation of specific CXCR4-ligand interaction at the cell membrane for fluorescence-based screening. Bioconjug Chem. 2008; 19:1917–20. [PubMed: 18707146]
48. van den Berg NS, Buckle T, Kuil J, Wesseling J, van Leeuwen FW. Immunohistochemical detection of the CXCR4 expression in tumor tissue using the fluorescent peptide antagonist Ac-TZ14011-FITC. Transl Oncol. 2011; 4:234–40. [PubMed: 21804919]
49. Kuil J, Steunenberg P, Chin PT, et al. Peptide-functionalized luminescent iridium complexes for lifetime imaging of CXCR4 expression. Chembiochem. 2011; 12:1897–903. [PubMed: 21739561]
50. Nishizawa K, Nishiyama H, Oishi S, et al. Fluorescent imaging of high-grade bladder cancer using a specific antagonist for chemokine receptor CXCR4. Int J Cancer. 2010; 127:1180–7. [PubMed: 20039317]
51. Zhang J, Fu Y, Li G, Zhao RY, Lakowicz JR. Detection of CXCR4 receptors on cell surface using a fluorescent metal nanoshell. J Biomed Opt. 2011; 16:016011. [PubMed: 21280917]
52. Huang X, Lee S, Chen X. Design of “smart” probes for optical imaging of apoptosis. Am J Nucl Med Mol Imaging. 2011; 1:3–17. [PubMed: 22514789]
53. Zhang Y, Hong H, Engle JW, et al. Positron emission tomography and near-infrared fluorescence imaging of vascular endothelial growth factor with dual-labeled bevacizumab. Am J Nucl Med Mol Imaging. 2012; 2:1–13. [PubMed: 22229128]
54. Meincke M, Tiwari S, Hattermann K, Kalthoff H, Mentlein R. Near-infrared molecular imaging of tumors via chemokine receptors CXCR4 and CXCR7. Clin Exp Metastasis. 2011; 28:713–20. [PubMed: 21735100]
55. van Dam GM, Themelis G, Crane LM, et al. Intraoperative tumor-specific fluorescence imaging in ovarian cancer by folate receptor-alpha targeting: first inhuman results. Nat Med. 2011; 17:1315–9. [PubMed: 21926976]
56. Liekens S, Schols D, Hatse S. CXCL12-CXCR4 axis in angiogenesis, metastasis and stem cell mobilization. Curr Pharm Des. 2010; 16:3903–20. [PubMed: 21158728]
57. Wang J, Loberg R, Taichman RS. The pivotal role of CXCL12 (SDF-1)/CXCR4 axis in bone metastasis. Cancer Metastasis Rev. 2006; 25:573–87. [PubMed: 17165132]
58. Luker KE, Gupta M, Luker GD. Imaging CXCR4 signaling with firefly luciferase complementation. Anal Chem. 2008; 80:5565–73. [PubMed: 18533683]
59. Luker KE, Gupta M, Luker GD. Imaging chemokine receptor dimerization with firefly luciferase complementation. FASEB J. 2009; 23:823–34. [PubMed: 19001056]
60. Luker K, Gupta M, Luker G. Bioluminescent CXCL12 fusion protein for cellular studies of CXCR4 and CXCR7. Biotechniques. 2009; 47:625–32. [PubMed: 19594447]
61. Luker KE, Mihalko LA, Schmidt BT, et al. In vivo imaging of ligand receptor binding with Gaussia luciferase complementation. Nat Med. 2012; 18:172–7. [PubMed: 22138753]
62. Ray P, Lewin SA, Mihalko LA, et al. Noninvasive imaging reveals inhibition of ovarian cancer by targeting CXCL12-CXCR4. Neoplasia. 2011; 13:1152–61. [PubMed: 22241961]
63. Luker KE, Lewin SA, Mihalko LA, et al. Scavenging of CXCL12 by CXCR7 promotes tumor growth and metastasis of CXCR4-positive breast cancer cells. Oncogene. 2012 Epub ahead of print.
64. Phelps ME, Hoffman EJ, Mullani NA, Ter-Pogossian MM. Application of annihilation coincidence detection to transaxial reconstruction tomography. J Nucl Med. 1975; 16:210–24. [PubMed: 1113170]
65. Gambhir SS, Czernin J, Schwimmer J, et al. A tabulated summary of the FDG PET literature. J Nucl Med. 2001; 42:1S–93S. [PubMed: 11483694]
66. Iagaru A. ^{18}F-FDG PET/CT: timing for evaluation of response to therapy remains a clinical challenge. Am J Nucl Med Mol Imaging. 2011; 1:63–4. [PubMed: 23133796]

67. De Saint-Hubert M, Brepoels L, Devos E, et al. Molecular imaging of therapy response with ^{18}F-FLT and ^{18}F-FDG following cyclophosphamide and mTOR inhibition. Am J Nucl Med Mol Imaging. 2012; 2:110–21. [PubMed: 23133806]
68. Hao G, Hajibeigi A, De León-Rodríguez LM, Öz OK, Sun X. Peptoid-based PET imaging of vascular endothelial growth factor receptor (VEGFR) expression. Am J Nucl Med Mol Imaging. 2011; 1:65–75. [PubMed: 23133797]
69. Sephton SM, Dennler P, Leutwiler DS, et al. Synthesis, radiolabelling and in vitro and in vivo evaluation of a novel fluorinated ABP688 derivative for the PET imaging of metabotropic glutamate receptor subtype 5. Am J Nucl Med Mol Imaging. 2012; 2:14–28. [PubMed: 23133799]
70. Donzella GA, Schols D, Lin SW, et al. AMD3100, a small molecule inhibitor of HIV-1 entry via the CXCR4 co-receptor. Nat Med. 1998; 4:72–7. [PubMed: 9427609]
71. Gerlach LO, Skerlj RT, Bridger GJ, Schwartz TW. Molecular interactions of cyclam and bicyclam non-peptide antagonists with the CXCR4 chemokine receptor. J Biol Chem. 2001; 276:14153–60. [PubMed: 11154697]
72. Weiss ID, Jacobson O, Kiesewetter DO, et al. Positron emission tomography imaging of tumors expressing the human chemokine receptor CXCR4 in mice with the use of ^{64}Cu-AMD3100. Mol Imaging Biol. 2012; 14:106–14. [PubMed: 21347799]
73. De Silva RA, Peyre K, Pullambhatla M, et al. Imaging CXCR4 expression in human cancer xenografts: evaluation of monocyclam ^{64}Cu-AMD3465. J Nucl Med. 2011; 52:986–93. [PubMed: 21622896]
74. Jacobson O, Weiss ID, Kiesewetter DO, Farber JM, Chen X. PET of tumor CXCR4 expression with 4–^{18}F-T140. J Nucl Med. 2010; 51:1796–804. [PubMed: 20956475]
75. Jacobson O, Weiss ID, Szajek LP, et al. PET imaging of CXCR4 using copper-64 labeled peptide antagonist. Theranostics. 2011; 1:251–62. [PubMed: 21544263]
76. Hennrich U, Seyler L, Schafer M, et al. Synthesis and in vitro evaluation of ^{68}Ga-DOTA-4-FBn-TN14003, a novel tracer for the imaging of CXCR4 expression. Bioorg Med Chem. 2012; 20:1502–10. [PubMed: 22264762]
77. Jacobson O, Weiss ID, Szajek LP, et al. Improvement of CXCR4 tracer specificity for PET imaging. J Control Release. 2012; 157:216–23. [PubMed: 21964282]
78. Gourni E, Demmer O, Schottelius M, et al. PET of CXCR4 expression by a ^{68}Ga-labeled highly specific targeted contrast agent. J Nucl Med. 2011; 52:1803–10. [PubMed: 22045709]
79. Demmer O, Dijkgraaf I, Schumacher U, et al. Design, synthesis, and functionalization of dimeric peptides targeting chemokine receptor CXCR4. J Med Chem. 2011; 54:7648–62. [PubMed: 21905730]
80. Aparici CM, Carlson D, Nguyen N, Hawkins RA, Seo Y. Combined SPECT and multidetector CT for prostate cancer evaluations. Am J Nucl Med Mol Imaging. 2012; 2:48–54. [PubMed: 22267999]
81. Ogasawara Y, Ogasawara K, Suzuki T, et al. Preoperative ^{123}I-iomazenil SPECT imaging predicts cerebral hyperperfusion following endarterectomy for unilateral cervical internal carotid artery stenosis. Am J Nucl Med Mol Imaging. 2012; 2:77–87. [PubMed: 23133803]
82. Hanaoka H, Mukai T, Tamamura H, et al. Development of a ^{111}In-labeled peptide derivative targeting a chemokine receptor, CXCR4, for imaging tumors. Nucl Med Biol. 2006; 33:489–94. [PubMed: 16720240]
83. Buckle T, van den Berg NS, Kuil J, et al. Non-invasive longitudinal imaging of tumor progression using an ^{111}indium labeled CXCR4 peptide antagonist. Am J Nucl Med Mol Imaging. 2012; 2:99–109. [PubMed: 23133805]
84. Nimmagadda S, Pullambhatla M, Pomper MG. Immunoimaging of CXCR4 expression in brain tumor xenografts using SPECT/CT. J Nucl Med. 2009; 50:1124–30. [PubMed: 19525448]
85. Misra P, Lebeche D, Ly H, et al. Quantitation of CXCR4 expression in myocardial infarction using ^{99m}Tc-labeled SDF-1alpha. J Nucl Med. 2008; 49:963–9. [PubMed: 18483105]
86. Kuil J, Buckle T, Yuan H, et al. Synthesis and evaluation of a bimodal CXCR4 antagonistic peptide. Bioconjug Chem. 2011; 22:859–64. [PubMed: 21480671]
87. Kuil J, Buckle T, Oldenburg J, et al. Hybrid peptide dendrimers for imaging of chemokine receptor 4 (CXCR4) expression. Mol Pharm. 2011; 8:2444–53. [PubMed: 22085282]

88. Cai W, Hong H. Peptoid and positron emission tomography: an appealing combination. Am J Nucl Med Mol Imaging. 2011; 1:76–9. [PubMed: 22022661]

89. Cai W, Olafsen T, Zhang X, et al. PET imaging of colorectal cancer in xenograft-bearing mice by use of an ^{18}F-labeled T84. 66 anti-carcinoembryonic antigen diabody. J Nucl Med. 2007; 48:304–10. [PubMed: 17268029]

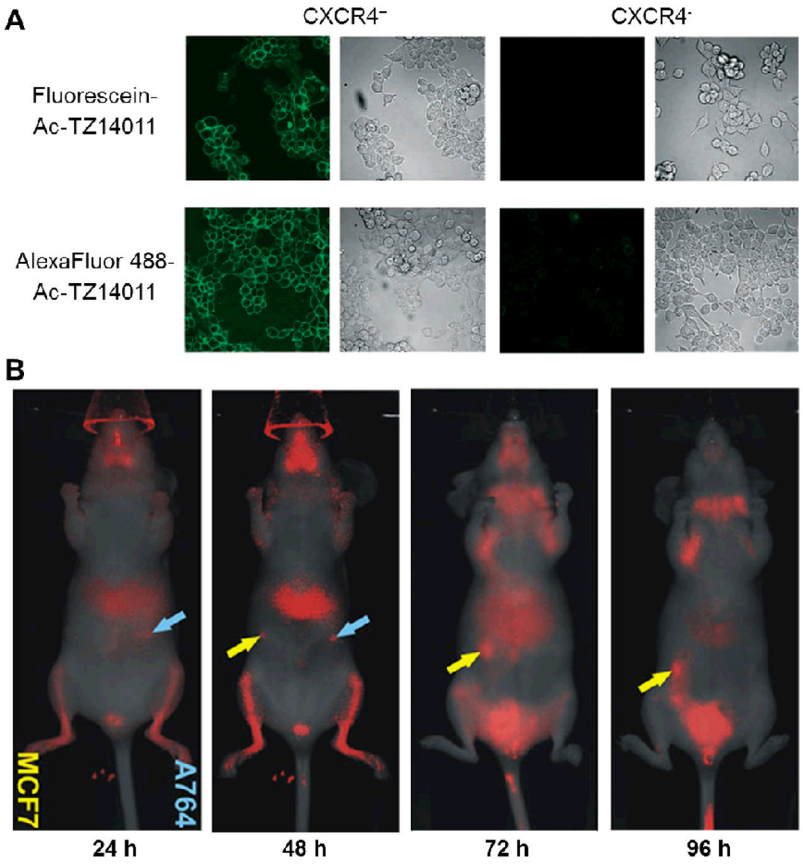

Fig. 1.

Fluorescence imaging of CXCR4. **A.** Confocal microscopy imaging of $CXCR4^+$ and $CXCR4^-$ cells using fluorescein- or AlexaFluor 488-labelled Ac-TZ14011. **B.** Serial *in vivo* imaging of mice implanted with MCF7 (yellow arrows) and A764 (cyan arrows) tumors after administration of IRDye 800CW-labelled CXCL12. Adapted from [46, 54].

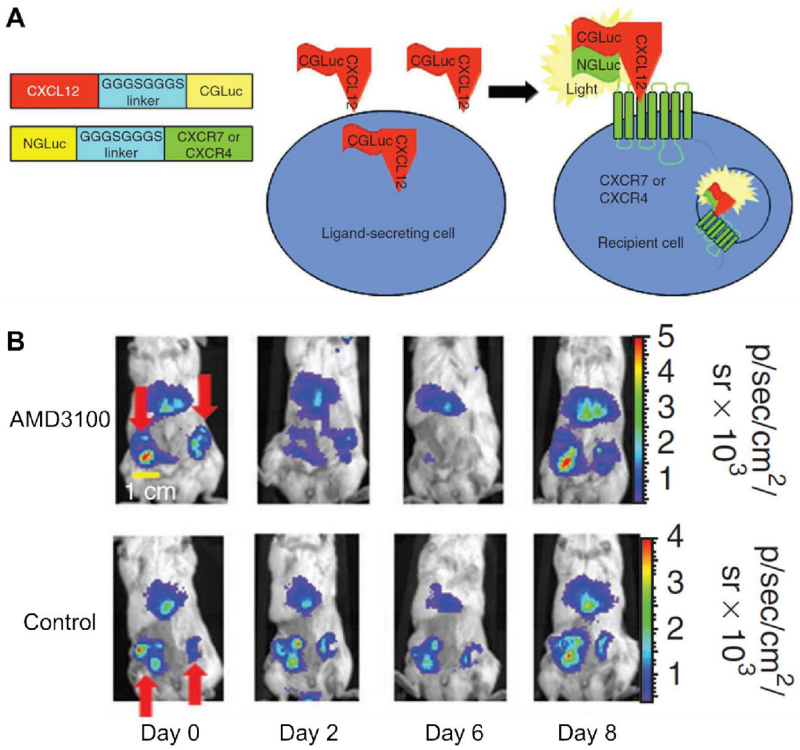

Fig. 2.

Bioluminescence imaging of CXCR4. **A.** A schematic diagram of the constructs, where binding of CXCL12-CGLuc to NGLuc-CXCR4 or NGLuc-CXCR7 reconstitutes GLuc and produces light. **B.** Images of mice before treatment (day 0), during treatment with AMD3100 or phosphate-buffered saline control (days 2 and 6), and after treatment (day 8). Red arrows point to the GLuc complementation signal in primary breast tumors. Adapted from [61].

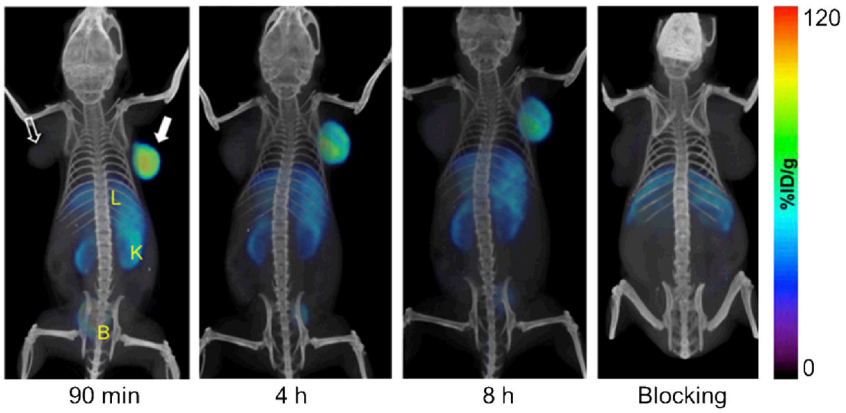

Fig. 3.

Serial PET/CT images of CXCR4 expression in subcutaneous brain tumor xenografts at 90 minutes, 4 h, and 8 h after injection of ^{64}Cu-AMD3465. “Blocking” denotes co-injection of the tracer with unlabelled AMD3465. The solid arrow indicates the U87-stb-CXCR4 tumor while the unfilled arrow indicates the wild-type U87 tumor. B: bladder; K: kidney; L: liver. Image adopted from [73].

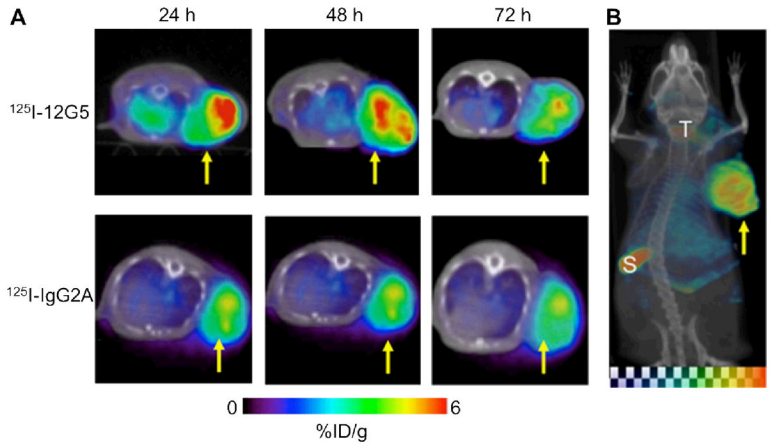

Fig. 4.

SPECT/CT of CXCR4 expression. **A.** Serial SPECT/CT images of severe combined immunodeficient mice bearing U87 glioblastoma xenografts, after injection with either ^{125}I-12G5 (an anti-human CXCR4 mAb) or ^{125}I-IgG2A (a control antibody) via tail vein. **B.** A maximum intensity projection image of a mouse injected with ^{125}I-12G5 at 48 h post-injection. %ID/g: percentage of injected dose per gram of tissue; S: spleen; T: thyroid. Arrows indicate the tumors. Adapted from [84].

Table 1

A tabulated summary of literature reports on molecular imaging of CXCR4.

Targeting Ligand	Imaging Label	Imaging Modality	References
T140	^{18}F	PET	[74]
	^{64}Cu	PET	[75]
	^{68}Ga	PET	[76]
	^{64}Cu	PET	[77]
Ac-TZ14011	Fluorescein/AlexaFluor 488	Fluorescence	[46]
	Fluorescein/TAMRA	Fluorescence	[47]
	Fluorescein	Fluorescence	[48]
	Iridium dye	Fluorescence	[49]
	^{111}In	SPECT	[82]
	^{111}In	SPECT	[83]
	^{111}In & CyAL-5.5	SPECT/Fluorescence	[86]
	^{111}In & CyAL-5.5	SPECT/Fluorescence	[87]
TY14003	Carboxyfluorescein	Fluorescence	[50]
CPCR4-2	^{68}Ga	PET	[35, 78]
AMD3100	^{64}Cu	PET	[38]
	^{64}Cu	PET	[39]
	^{64}Cu	PET	[72]
AMD3465	^{64}Cu	PET	[73]
Anti-CXCR4	Metal nanoshells	Fluorescence	[51]
mAb	^{125}I	SPECT	[84]
SDF-1/CXCL12	Fluorescein	Fluorescence	[45]
	IRDye 800CW	Fluorescence	[54]
	FLuc	Bioluminescence	[58]
	FLuc	Bioluminescence	[59]
	GLuc	Bioluminescence	[60]
	GLuc	Bioluminescence	[61]
	GLuc & FLuc	Bioluminescence	[62]
	GLuc & FLuc	Bioluminescence	[63]
	^{99m}Tc	SPECT	[85]